2023 IEEE International Conference on Robotics and Automation (ICRA 2023)
May 29 - June 2, 2023. London, UK

Robust Output Feedback controller for a Serial Robotic Manipulator with Unknown Nonlinearities and External Disturbances

Mohammad Al Saaideh Almuatazbellah M. Boker Mohammad Al Janaideh

***Abstract*— This paper presents a robust output feedback controller for a n-link serial robotic manipulator with unknown dynamics and external disturbances. First, the robotic manipulator's model is formulated with unknown dynamics, including joint coupling, nonlinearities, and external disturbances. Second, an output feedback controller is proposed by combining a backstepping controller and an extended high-gain observer to estimate the unknown dynamic and external disturbances in addition to the system states. Experiments on 4 DOF robotic manipulators verify the proposed control approach. The proposed control approach achieved the end-effector's desired trajectory under unknown system dynamics and disturbances.**

I. Introduction

In recent years, robotic manipulators have played an important role in automating trade, engineering, medicine, space exploration, and ocean exploration. Advanced controllers must be able to perform high-productivity, high-accuracy tasks under various working conditions, such as external disturbances, measurement errors, or unknown dynamics. They must also be able to provide smooth, safe, and dependable control in a variety of working environments. Obtaining an accurate robotic manipulator dynamic model is difficult due to the complex nonlinearities, joint coupling, and parameter uncertainty. This leads to a challenging research problem in achieving high precision and robustness in the presence of nonlinearities, uncertainties and external disturbances.

The control system for robotic manipulators aims to make the end-effector follow a desired trajectory path. The design of the control system for the robotic manipulators includes first determining the expected motion of the joints using the inverse kinematics based on the desired trajectory path of the end-effector. Second, design a closed-loop control system to adjust the torque of the joints to achieve the desired motion [1], [2]. Different control methodologies have been used to design the closed-loop control system, which deals with different nonlinearities, uncertainties, and external disturbances of the robotic manipulators. The control methodologies include for example, PID control [3], optimal control [4], adaptive control [5]–[7], model predictive control [8], and intelligent control system based reinforcement learning [9]. Among the different control methodologies, the sliding mode control (SMC) has been widely used to deal with uncertainties and disturbances due to its robustness, see for example, [10]–[12]. However, the main disadvantage of the SMC is the chattering behaviour in the control signal, which leads to singularities issues and practical implementation issues, including high friction of mechanical parts and high heat in electrical components [13]. Different improvements have been considered to overcome the limitations of SMC, such as terminal SMC [14] and fast terminal SMC [11]. In addition to designing the robust controller, state and disturbance observers can be designed to estimate the robotic manipulator's unknown dynamics and external disturbances to improve the performance of the closed-control system [15], [16]. The extended high gain observer (EHGO) has been widely used to estimate the unknown dynamic and external disturbances for a nonlinear dynamic system [17]. The EHGO can estimate all states of the dynamic system, modelling uncertainties and external disturbances; in addition, the EHGO allows recovery of the state feedback controller's performance and shapes the transient performance of the closed-loop system [17].

In this work, we find a solution for the position-tracking control of a robotic manipulator whose nonlinear dynamics are unknown and are subject to exogenous disturbances. In particular, we achieve trajectory tracking for n-joint robotic manipulators with unknown nonlinearities, uncertainties, joint dynamic couplings, and external disturbances. For this purpose, we develop an output feedback control system that combines backstepping controllers with high-gain observers. Compared to the other control approaches such as [11], [18], [19], the proposed control approach considers the system's dynamic to be totally unknown instead of the nominal model with uncertainties, and it can be tailored specifically for each joint with fewer tuning parameters. The proposed controller is evaluated on a four-joint robotic manipulator, which is a departure from the two-joint robotic manipulators typically used in the literature.

II. Output Feedback Control Approach

A. Problem Formulation

The dynamic model of the n-link rigid robotic manipulator can be given as [20]

$$M(q)\ddot{q} + C(q,\dot{q}) + G(q) = \mathcal{T} + \mathcal{T}_d \tag{1}$$

where $q, \dot{q}, \ddot{q} \in \mathbb{R}^n$ are the vectors of the joint position, velocity and acceleration, respectively, $M(q)$ is the inertial matrix, $C(q,\dot{q})$ is the Coriolis matrix, $G(q)$ is the gravity

M. Al Saaideh and M. Al Janaideh are with Department of Mechanical and Mechatronics Engineering, Memorial University, St. John's, NL A1B 3X5, Canada. mialsaaideh@mun.ca, maljanaideh@mun.ca, M. Al Janaideh is with the School of Engineering, University of Guelph, Guelph, ON N1G 2W1, Canada maljanai@uoguelph.ca

M. Boker iw with Bradley Department of Electrical and Computer Engineering, Virginia Tech, Blacksburg, VA 24060, USA. boker@vt.edu

matrix, $\mathcal{T}$ is the input torque of the joint, and $\mathcal{T}_d$ is the external-bounded disturbance on the joint.

The inertia matrix of the system can be rewritten as $M(q) = M_o + M_1(q)$, where M_o is related to constant parameters related to the geometry of the manipulator and the term $M_1(q)$ is related to the joint coupling and nonlinearities. Typically, $M_1(q)$, $C(q,\dot{q})$ and $G(q)$ are complex to be obtained due to measurement error, unknown dynamic coupling, external environmental disturbances, and parameters uncertainties, which can be considered as unknown dynamics [12]. Motivated by this, the dynamic model can be rewritten as

$$M_o\ddot{q} = F(q,\dot{q},\ddot{q}) + \mathcal{T} + \mathcal{T}_d \tag{2}$$

where $M_o = \text{diag}[\mu_1, \cdots, \mu_n]_{n\times n}$ are constants related to the manipulator's geometry, $F(q,\dot{q},\ddot{q}) = -M_1(q)\ddot{q} - C(q,\dot{q}) - G(q)$, is a bounded function representing the unknown dynamic due to nonlinearities and joint coupling. Defining the state variable as $\eta_{k1} = \theta_k$ and $\eta_{k2} = \dot{\theta}_k$ allows to express the dynamic model for each joint $k \in \{1,\ 2,\ 3, \cdots, n\}$ as

$$\begin{bmatrix}\dot{\eta}_{k1}\\ \dot{\eta}_{k2}\end{bmatrix} = \begin{bmatrix}0 & 1\\ 0 & 0\end{bmatrix}\begin{bmatrix}\eta_{k1}\\ \eta_{k2}\end{bmatrix} + \begin{bmatrix}0\\ \frac{1}{\mu_k}\end{bmatrix}u_k + \begin{bmatrix}0\\ 1\end{bmatrix}\psi_k + \begin{bmatrix}0\\ 1\end{bmatrix}\delta_k, \tag{3}$$

$$y_k = \eta_{k1}, \tag{4}$$

where $u_k = \mathcal{T}_k$ is the applied torque of the joint k, $\psi_k = F_k/\mu_k$ is the unknown dynamic of the joint k, and $\delta_k = \mathcal{T}_{dk}/\mu_k$ is the external disturbance acting on the joint k.

The objective is to design a controller such that the output at each joint $y_k(t) = \theta_k(t)$ tracks a desired reference signal $r_{k1}(t)$ under unknown nonlinearity ψ_k and unknown external disturbances δ_k. All derivatives $(\dot{r}_{k1}, \ddot{r}_{k1})$ are piecewise continuous and bounded for all $t \geq 0$. Towards accomplishing this objective, we consider the change of variables $e_{k1} = \eta_{k1} - r_{k1}$, $e_{k2} = \eta_{k2} - r_{k2}$ where r_{k2} is desired signal to be designed such that the origin ($e_{k1} = 0$, $e_{k2} = 0$) is exponentially stable.

B. Backstepping Controller

The state feedback controller design follows the design procedures of backstepping [21]. In state feedback tracking controllers, variables are changed to transform an original system into an error coordinate system with an equilibrium at the origin. A state feedback control is then designed so that the origin of the transferred system is exponentially stable to achieve the desired tracking result. Consider a tracking error of θ_{k1} defined as $e_{k1} = \eta_{k1} - r_{k1}$ and $e_{k2} = \eta_{k2} - r_{k2}$ such that

$$\dot{e}_{k1} = \eta_{k2} - \dot{r}_{k1}, \tag{5}$$

$$\dot{e}_{k2} = \frac{1}{\mu_k}u_k + \psi_k + \delta_k - \dot{r}_{k2}. \tag{6}$$

Define $r_{k2} = -\alpha_{k1}e_{k1} + \dot{r}_{k1}$, where $\alpha_{k1} > 0$ is a positive constant to be designed. Then, the system (5)-(6) can be rewritten as

$$\dot{e}_{k1} = -\alpha_{k1}e_{k1} + e_{k2}, \tag{7}$$

$$\dot{e}_{k2} = \frac{1}{\mu_k}u_k + \psi_k + \delta_k - \dot{r}_{k2}, \tag{8}$$

where $\dot{r}_{k2} = -\alpha_{k1}\dot{e}_{k1} + \ddot{r}_{k1}$. The control objective, now, is to design a state feedback control to stabilize the system (7)-(8). Towards this goal, suppose there is a control law u_k that can be designed to stabilize the origin ($e_{k1} = 0$, $e_{k2} = 0$). For this purpose, consider a smooth and positive definite Lyapunov function candidate as

$$V_k = \frac{1}{2}e_{k1}^2 + \frac{1}{2}e_{k2}^2. \tag{9}$$

where the derivative of V along the systems (7)-(8) can be expressed by

$$\begin{aligned}\dot{V}_k =& e_{k1}\dot{e}_{k1} + e_{k2}\dot{e}_{k2} = e_{k1}\left(-\alpha_{k1}e_{k1} + e_{k2}\right)\\ &+ e_{k2}\left(\frac{1}{\mu_k}u_k + \psi_k + \delta_k - \dot{r}_k\right).\end{aligned} \tag{10}$$

The control signal u_k should be designed to make $\dot{V}$ strictly negative. Thus, the control law can be selected as $u_k \triangleq \Gamma_k(e_{k1}, e_{k2}, \sigma_k, r_k)$, with

$$\Gamma_k = \mu_k\left(-\alpha_{k2}e_{k2} - e_{k1} + \dot{r}_{k2} - \sigma_k\right), \tag{11}$$

where $\alpha_{k2} > 0$ and $\beta_k > 0$ are positive constants to be selected, and $\sigma_k = \psi_k + \delta_k$. With the proposed control signal u_k, (7)-(8) can be written as

$$\begin{aligned}\begin{bmatrix}\dot{e}_{k1}\\ \dot{e}_{k2}\end{bmatrix} =& \begin{bmatrix}-\alpha_{k1} & 1\\ -1 & -\alpha_{k2}\end{bmatrix}\begin{bmatrix}e_{k1}\\ e_{k2}\end{bmatrix},\\ \dot{e}_k =& f_k(e_k, u_k - \Gamma_k(e_{k1}, e_{k2}, \sigma_k, r_k)),\end{aligned} \tag{12}$$

where $e_k = \begin{bmatrix}e_{k1}, & e_{k2}\end{bmatrix}^T$. Then the derivative of the Lyapunov function along the system (12) satisfies

$$\dot{V}_k = -\alpha_{k1}e_{k1}^2 - \alpha_{k2}e_{k2}^2, \tag{13}$$

$$\dot{V}_k = -e_k^T Q_k e_k, \tag{14}$$

where $Q_k = \begin{bmatrix}\alpha_{k1} & 0\\ 0 & \alpha_{k2}\end{bmatrix}$. Thus, it can be shown that

$$\dot{V}_k \leq -\lambda_{\max}(Q_k)\|e_k\|^2, \tag{15}$$

which implies that the origin of the system (12) is exponentially stable.

C. The Extended High-gain Observer

The extended high-gain observer (EHGO) can estimate the unknown system dynamic due to modelling errors, uncertainties in dynamic parameters, and unknown disturbances [17], [22]. For robotic manipulator, the EHGO uses the measured joint angle $y_k = \theta_k = \eta_{k1}$ to estimate the joint's velocity η_{k2} and unknown dynamics of the joint ψ_k. The EHGO is formulated as

$$\dot{\hat{\eta}}_{k1} = \hat{\eta}_{k2} + \frac{\gamma_{k1}}{\epsilon_k}(y_k - \hat{\eta}_{k1}), \tag{16}$$

$$\dot{\hat{\eta}}_{k2} = \frac{1}{\mu_k}u_k + \hat{\sigma}_k + \frac{\gamma_{k2}}{\epsilon_k^2}(y_k - \hat{\eta}_{k1}), \tag{17}$$

$$\dot{\hat{\sigma}}_k = \frac{\gamma_{k3}}{\epsilon_k^3}(y_k - \hat{\eta}_{k1}), \tag{18}$$

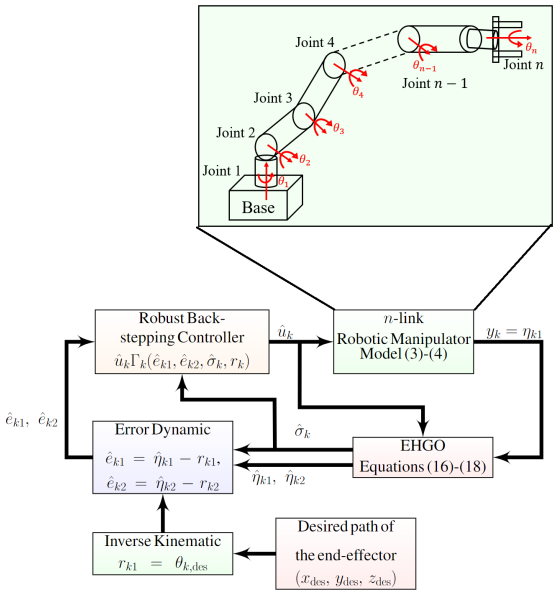

Fig. 1: Schematic diagram of the closed-loop output feedback control system of n-link robotic manipulator.

where γ_{k1}, γ_{k2} and γ_{k3} are chosen such that the polynomial $s^3+\gamma_{k1}s^2+\gamma_{k2}s+\gamma_{k3}=0$ is Hurwitz. The dynamic errors can be expressed as $\hat{e}_{k1}=\hat{\eta}_{k1}-r_{k1}$ and $\hat{e}_{k2}=\hat{\eta}_{k2}-r_{k2}$.

D. Output Feedback Control

The robust state feedback controller is combined with the EHGO to solve the robotic manipulator's output-feedback control problem of trajectory tracking. Accordingly, the output-feedback control using the estimated states as

$$u_k=\pm S_k\text{sat}\left(\frac{\Gamma(\hat{e}_{k1},\hat{e}_{k2},\hat{\sigma}_k,r_k)}{S_k}\right), \tag{19}$$

where the control law Γ is defined in (11), and $\text{sat}(.)$ is the saturation function which is used to protect the system from peaking in the observer's transient response [23]. The saturation limit S_k is chosen to based on the practical physical constraints of the maximum torque that can be achieved from the motor. The structure of the closed-loop system with the proposed output-feedback controller is illustrated in Figure 1. To analyze the performance of the closed-loop system, consider the following scaled estimation errors

$$\phi_{k1}=(\eta_{k1}-\hat{\eta}_{k1})/\epsilon_k^2,\quad \phi_{k2}=(\eta_{k2}-\hat{\eta}_{k2})/\epsilon_k,\quad \phi_{k3}=\sigma_k-\hat{\sigma}_k,$$

such that the closed-loop system under output feedback can be expressed as

$$\dot{e}_k=f_k(e_k,u_k-\Gamma_k(\hat{e}_{k1},\hat{e}_{k2},\hat{\sigma}_k,r_k)), \tag{20}$$

$$\epsilon_k\dot{\phi}_k=\Lambda_k\phi_k+\epsilon_k\begin{bmatrix}0\\0\\1\end{bmatrix}\dot{\sigma}_k, \tag{21}$$

where $\phi_k=\begin{bmatrix}\phi_{k1} & \phi_{k2} & \phi_{k2}\end{bmatrix}^T$, $\Lambda_k=\begin{bmatrix}-\gamma_{k1} & 1 & 0\\ -\gamma_{k2} & 0 & 1\\ -\gamma_{k3} & 0 & 0\end{bmatrix}$.

The closed-loop system (20)-(21) is in the standard singularly perturbed form with a two-time scale structure. The slow variable is $e_k(t)$ and the fast variables are $\phi_k(t)$. By setting $\epsilon_k=0$ in (21), $\phi_k=0$ and we get the reduced system (12) and this implies the following theorem.

Theorem 1: Consider the closed-loop system formed of the system (3)-(4), the observer (16)-(18), and the controller (19). Let $(e_{k1},\ e_{k2})\in\mathcal{M}$ and $(\eta_{k1}(0),\ \eta_{k2}(0),\ \psi_k(0))\in\mathcal{N}$, where $\mathcal{M}$ and $\mathcal{N}$ are any given compact subsets of $\mathbb{R}^{2k}$ and $\mathbb{R}^{3k}$, respectively, then we have: (i) **boundedness:** there exists $\epsilon_a>0$ such that for every $0<\epsilon_k<\epsilon_a$, the trajectories of the closed-loop system are bounded for all $t>0$, (ii) **stability:** there exists $\epsilon_b>0$ such that, for every $0<\epsilon_k\le\epsilon_b$, the origin of the closed-loop system (20)-(21) is exponential stable and $\mathcal{M}\times\mathcal{N}$ is a subset of its region of attraction, and (iii) **performance recovery:** given any $\lambda>0$, there exist $\epsilon_c>0$, dependent on λ, such that for every $0<\epsilon_k<\epsilon_c$,

$$\|e_k(t,\epsilon_k)-e_{kd}(t)\|\le\lambda \tag{22}$$

where $e_k(t,\epsilon)$ is the solution of the system (20)-(21), $e_{kd}(t)$ is the solution of the system (12) starting from $e_k(0)=0$.

Proof: The proof follows the singular perturbation approach and uses similar arguments and the proof of Theorem 3.1 in [23]. Consider a new timescale as $\tau=t/\epsilon_k$ such that the system (20)-(21) can be rewritten as the following boundary layer subsystem

$$\frac{de_k}{d\tau}=\epsilon_k(e_k,u_k-\hat{\Gamma}_k(\hat{e}_{k1},\hat{e}_{k2},\hat{\sigma_{kk}},r_k)), \tag{23}$$

$$\frac{d\phi}{d\tau}=\Lambda\phi+\epsilon_k\begin{bmatrix}0\\0\\1\end{bmatrix}\dot{\sigma}_k, \tag{24}$$

setting $\epsilon_k=0$ in this time scale yields to $\frac{d\phi}{d\tau}=\Lambda\phi$.

For this boundary layer subsystem, the Lyapunov function $V_a(\phi_k)=\phi_k^TP_a\phi_k$, where P_a is the positive definite solution of the Lyapunov equation $P_a\Lambda_k+\Lambda_k^TP_a=-I$, satisfies $\lambda_{\min}(P_a)\|\phi_k\|^2\le V_a(\eta)\le\lambda_{\max}(P_a)\|\phi_k\|^2$, and $\frac{\partial V_a}{\partial\phi_k}[\Lambda_0\phi_k]\le-\|\phi_k\|^2$.

Let $\mathcal{S}=\{V_k(e_k)\le\rho\}\times\{V_a(\phi_k)\le\rho_a\epsilon_k^2\}$, where V_k is defined in (9), and ρ_a are positive constants to be specified. We will show that $\mathcal{S}$ is positively invariant set for every $0<\epsilon_k\le\epsilon_a$, for some $\epsilon_a>0$. The function σ is a smooth locally Lipschitz, and it can be considered that $\dot{\sigma_k}\le L_1\|\phi_k\|$, thus the derivative of V_a along the system (21) can be expressed as

$$\epsilon_k\dot{V}_a\le-\|\phi_k\|^2+2\epsilon_kL_1\|P_a\|\|\phi_k\|,$$

For any value of $\epsilon_{a1}>0$ and $\rho_a=4L_1^2\|P_a\|^2\ \lambda_{\max}(P_a)$, it can be shown that

$$\epsilon_k\dot{V}_a\le-\frac{1}{2}\|\phi_k\|^2\quad\forall\quad\|\phi_k\|\ge(4L_1\|P_a\|)\epsilon_k \tag{25}$$

for $0\le\epsilon_k\le\epsilon_{a1}$ and $\mathcal{S}=\{V_k(e_k)\le\rho\}\times\{V_a(\phi_k)=\rho_a\epsilon_k^2\}$. For the system (20), the derivative of V_k can be presented as

$$\dot{V}_k\le-\lambda_{\max}(Q_k)\|e_k\|^2+c_1L_2\|\phi_k\|, \tag{26}$$

where c_1 is the upper bound of (dV_k/de_k), L_2 is Lipschitz constant, and $\|\phi_k\|\le\sqrt{\rho_a/\lambda_{\min}(P_a)}\epsilon_k$. Taking $\epsilon_{a2}=\rho_b/(c_1L_2\sqrt{\rho_a/\lambda_{\min}(P_a)})$ where $\rho_b=$

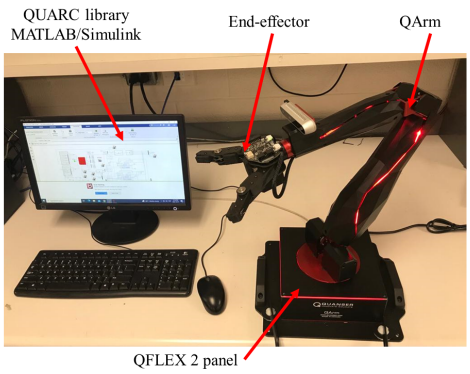

(a)

Fig. 2: Experimental setup of the QArm system from Quanser.

$\min_{e_k \in \partial\Omega}(\left[\lambda_{\max}(Q_k)\|e_k\|^2\right])$, we can show that $\dot{V}_k \leq 0$ for $0 \leq \epsilon \leq \epsilon_{a2}$ and $\mathcal{S} = \{V_k(e_k) = \rho\} \times \{V_a(\phi_k) \leq \rho_a \epsilon_k^2\}$. Choose $\epsilon_a = \min\{\epsilon_{a1}, \epsilon_{a2}\}$, then it can be seen that, for all $0 < \epsilon_k \leq \epsilon_a$, $\mathcal{S}$ is positively invariant. Using a similar analysis to [23], then the trajectories of the closed-loop system (20)-(21) starting in the set $\mathcal{M}$ and $\mathcal{N}$ enter a positively invariant set $\mathcal{S}$ dependent on ϵ_k in a finite time. The proof of (ii) and (iii) can be shown using similar arguments to the proof of Theorem 3.1 of [23]. ■

Remark 1: Theoreom 1 shows that the output feedback controller with the proposed EHGO (16)-(18) can exponentially recover the trajectories of the system (20)-(21). Practically, this is very beneficial. First, the designer can select e_k small enough such the estimation error is very small, which allows assuming all the states η_{k1}, η_{k2}, and nonlinear function σ_k are available for the state feedback controller. Second, this allows designing a control signal u_k to satisfy certain performance requirements in the state feedback design stage for any given initial conditions.

III. Case Study: 4 DOF Serial Robotic Manipulator

In this work, a four-joint robotic manipulator (roll-pitch-pitch-roll) is studied. Based on the Lagrangian equation, the nonlinear dynamic model of the 4-DOF robotic manipulator is given as [24]

$$(M_o + M)\ddot{\theta}_k + B(\theta)\dot{\theta}_i\dot{\theta}_j + C(\theta)\theta_k^2 + G(\theta) = \mathcal{T}_k, \quad (27)$$

where $i, j \in \{(1,2),\ (1,3),\ (1,4),\ (2,3),\ (2,4),\ (3,5)\}$, $k \in \{1,\ 2,\ 3,\ 4\}$, M_0 is the inertia constant matrix, M is the inertia matrix, B is the Coriolis matrix, C is the Centrifugal matrix, G is the gravity matrix. More details about the system model are given in the Appendix. In this work, the unknown nonlinearities and the dynamic coupling at each joint k is given as $\psi_k = -\frac{1}{\mu_k}\left(-M\ddot{\theta} - B(\theta)\dot{\theta}_i\dot{\theta}_j - C(\theta)\theta_k^2 - G(\theta)\right)$. Considering the states are defined as $\theta_k = \eta_{k1}$ and $\dot{\theta}_k = \eta_{k2}$, the dynamic equations of for each joint k can be rewritten by

$$\begin{bmatrix}\dot{\eta}_{k1}\\ \dot{\eta}_{k2}\end{bmatrix} = \begin{bmatrix}0 & 1\\ 0 & 0\end{bmatrix}\begin{bmatrix}\eta_{k1}\\ \eta_{k2}\end{bmatrix} + \begin{bmatrix}0\\ \frac{1}{\mu_k}\end{bmatrix}u_k + \begin{bmatrix}0\\ 1\end{bmatrix}\psi_k + \begin{bmatrix}0\\ 1\end{bmatrix}\delta_k, \quad (28)$$

$$y_k = \eta_{k1}, \quad (29)$$

where δ_k is the external disturbances on the joint k, and $u_k = \mathcal{T}_k$ is the applied torque on the joint k.

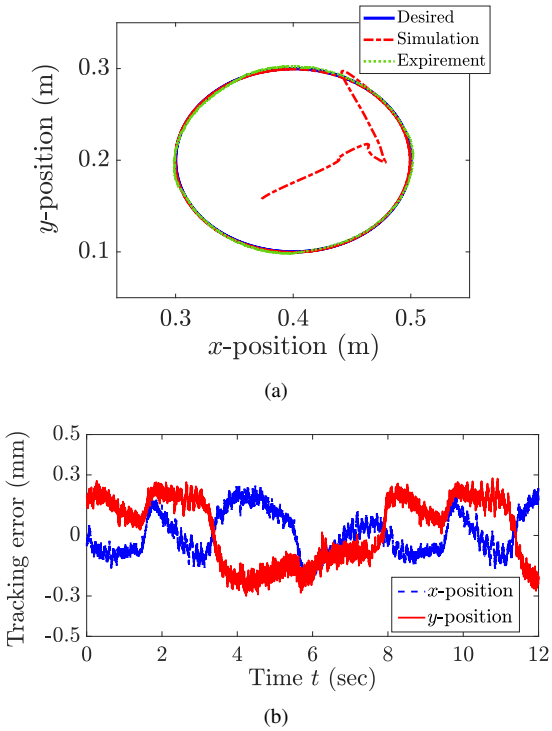

(a)

(b)

Fig. 3: Experimental results of (a) the trajectory path tracking of the end-effector and (b) the tracking errors of the end-effector.

A. Experimental results

The experimental tests for further validation of the practical control performances are carried out on QArm [24]. QArm is a 4-DOF serial manipulator from Quanser for research in a lab environment. The arm is configured using the QFLEX 2 panel, which allows control and access from a computer via a USB connection. The real-time controller for QArm is developed using the QUARC library in MATLAB/Simulink environment. The schematic diagram of the experimental setup and the geometry of the QArm are presented in Figure 2. Due to the difference between the actual parameters of QArm and the parameters that are considered in the simulation, the controller and the observer parameters are tuned to obtain the best results. The parameters of the controller and the observer for experimental tests are chosen for joint 1 ($k = 1$) as $\alpha_{11} = 1$, $\alpha_{12} = 2$, $\epsilon_1 = 0.075$ $\gamma_{11} = 40$, $\gamma_{12} = 20$, $\gamma_{13} = 30$, for joint 2 ($k = 2$) as $\alpha_{21} = 1.5$, $\alpha_{22} = 3$, $\epsilon_2 = 0.075$, $\gamma_{21} = 15$, $\gamma_{22} = 3$, $\gamma_{23} = 15$, and for joint 3 ($k = 3$) as $\alpha_{31} = 2.75$, $\alpha_{32} = 1.75$,

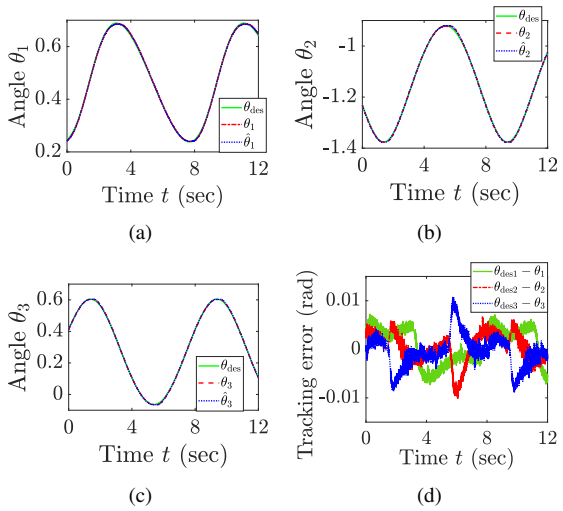

Fig. 4: Experimental results of the motion tracking of the joint angles (a) joint 1 (θ_1), (b) joint 2 (θ_2), (c) joint 3 (θ_3), and (d) the tracking error of the joint angles.

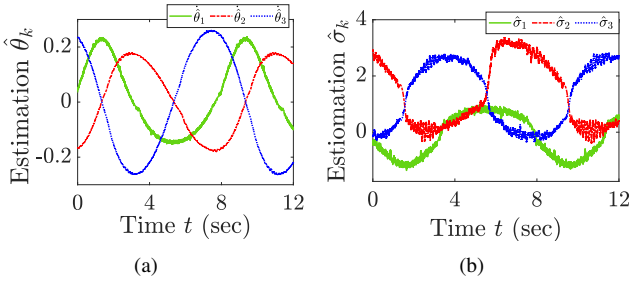

Fig. 5: Experimental results of the motion tracking of the joint angles (a) the estimation of the joints velocities $\hat{\dot{\theta}}_k$ and (b) the estimation of the unknown function $\hat{\sigma}_k$.

$\epsilon_3 = 0.1$, $\gamma_{31} = 50$, $\gamma_{32} = 10$, $\gamma_{33} = 50$. The ratio between the output control signal u_k and the motor voltage (PWM) v_k is considered as $v_k = \xi_k u_k$, where ξ_k are chosen as $\xi_1 = 0.085$, $\xi_2 = 0.065$, and $\xi_3 = 0.075$. The saturation limits for the control signal S_k are determined based on the maximum torque for the motor at each joint as $S_1 = \pm 15$, $S_2 = \pm 15$, and $S_3 = \pm 7$. The desired path of the end-effector is $x(t) = 0.4 + 0.1\sin(2\pi ft)$ and $y(t) = 0.2 + 0.1\cos(2\pi ft)$ with $f = 0.125$ Hz. Figure 3 shows the trajectory tracking of the end-effector. It is observed that the proposed output feedback controller achieves the desired trajectory path with a tracking error of less than 3% of the desired value. The motion tracking of the joint angles is illustrated in Figure 4, indicating the tracking errors of angles are less than 0.01 rad for all joints, as shown in Figure 4(d). Finally, the estimated velocities $\hat{\dot{\theta}}_k$ and the unknown function $\hat{\sigma}_k$ from the designed EHGO are illustrated in Figure 5(a) and (b), respectively.

B. Disturbance rejection

The robustness of the proposed control approach is verified by applying an external disturbance of $\delta_k = \sin(2\pi ft)$ with $f = 0.75$ Hz at joint k, which is added to the control

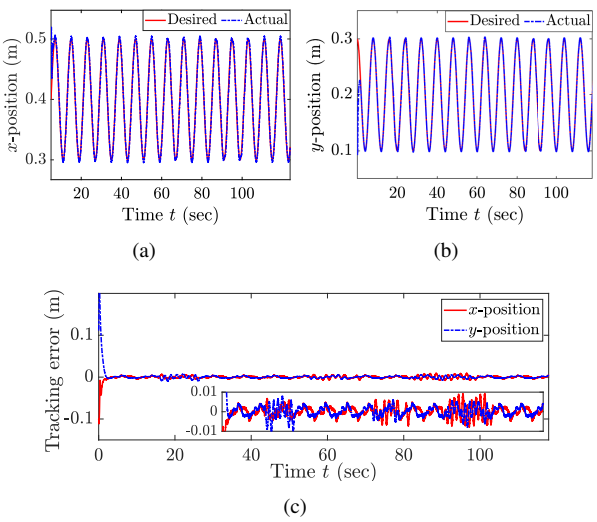

Fig. 6: Experimental results of the trajectory path of the end-effector under external disturbances (a) x-position,(b) y-position, and (c) tracking errors.

signal, then the experimental results are obtained. Figure 6 shows the tracking performances of the end-effector in x-position and y-position, and Figure 7 shows the motion tracking of the joints under external disturbances. It can be observed that under the disturbances at all joints, the proposed controller achieves the desired trajectory path with error amplitude less than 0.01 m as illustrated in Figure 6(c). Figure 8(a-c) show the estimation of the nonlinear function σ_k under different external disturbances δ_k. It is observed that the EHGO can estimate the disturbances as part of the nonlinear function σ_k. Figure 8(d-f) show the control signal u_k applied on each joint. These figures indicate that the controller uses the estimation of σ_k to generate a signal to reject the disturbances and achieve the desired trajectory.

IV. Conclusions

This work combines the backstepping controller and extended high gain observer (EHGO) for the n-link robotic manipulator with unknown dynamics and external disturbances. The backstepping controller is designed by selecting the controller's gains to achieve exponential stability with desired transient performances. The EHGO sequentially is used to estimate the states, the unknown dynamics and the external disturbances to improve the controller's robustness. The proposed control approach is a joint-specific controller with few parameters. The developed controller is tested on a Quanser industrial robotic manipulator, a 4-DOF serial robotic manipulator with a complex nonlinear dynamic model. Experimental results showed that the proposed controller could achieve the desired trajectory with less than 3% error for a system without disturbances and less than 9% under bounded external disturbances. The EHGO accurately estimates the unknown dynamics of robotic manipulators with external disturbances and provides robustness to the control system.

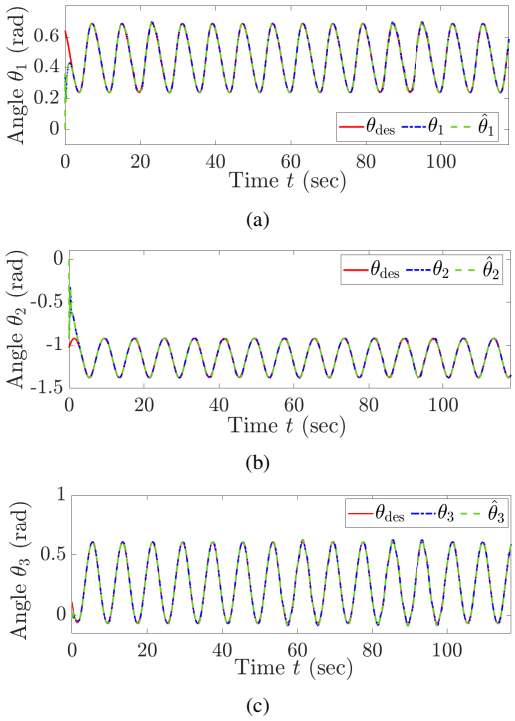

Fig. 7: Experimental results of the motion tracking under external disturbances (a) joint 1 (θ_1), (b) joint 2 (θ_2), and (c) joint 3 (θ_3).

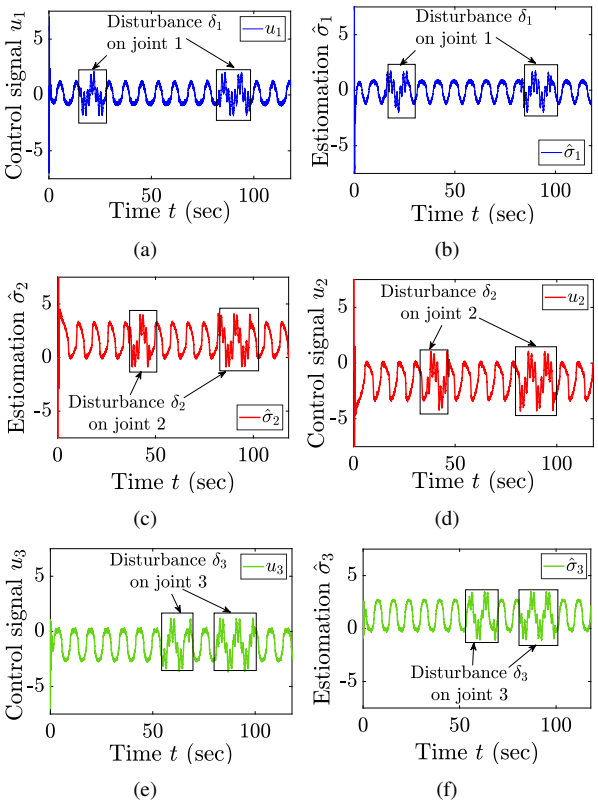

Fig. 8: Experimental results under external disturbances (a, c, and e) the control signal u_k, and (b, d, and f) the estimation of the unknown function $\hat{\sigma}_k$.

REFERENCES

[1] D. Zhang and B. Wei, "A review on model reference adaptive control of robotic manipulators," *Annual Reviews in Control*, vol. 43, pp. 188–198, 2017.

[2] M. Spong, "An historical perspective on the control of robotic manipulators," *Annual Review of Control, Robotics, and Autonomous Systems*, vol. 5, pp. 1–31, 2022.

[3] H. Nohooji, "Constrained neural adaptive pid control for robot manipulators," *Journal of the Franklin Institute*, vol. 357, pp. 3907–3923, 2020.

[4] H. Pan and M. Xin, "Nonlinear robust and optimal control of robot manipulators," *Nonlinear Dynamics*, vol. 76, pp. 237–254, 2014.

[5] C. Pezzato, R. Ferrari, and C. Corbato, "A novel adaptive controller for robot manipulators based on active inference," *IEEE Robotics and Automation Letters*, vol. 5, pp. 2973–2980, 2020.

[6] A. Menon, R. Prakash, and L. Behera, "Adaptive critic based optimal kinematic control for a robot manipulator," in *Proceedings of the International Conference on Robotics and Automation*, Montreal, QC, 2019, pp. 1316–1322.

[7] G. Garofalo, X. Wu, and C. Ott, "Adaptive passivity-based multi-task tracking control for robotic manipulators," *IEEE Robotics and Automation Letters*, vol. 6, pp. 7129–7136, 2021.

[8] M. Elsisi, K. Mahmoud, M. Lehtonen, and M. Darwish, "Effective nonlinear model predictive control scheme tuned by improved NN for robotic manipulators," *IEEE Access*, vol. 9, pp. 64 278–64 290, 2021.

[9] T. Thuruthel, E. Falotico, F. Renda, and C. Laschi, "Model-based reinforcement learning for closed-loop dynamic control of soft robotic manipulators," *IEEE Transactions on Robotics*, vol. 35, pp. 124–134, 2018.

[10] W. Qi, G. Zong, and H. Karimi, "Sliding mode control for nonlinear stochastic semi-markov switching systems with application to srmm," *IEEE Transactions on Industrial Electronics*, vol. 67, pp. 3955–3966, 2019.

[11] T. Truong, A. Vo, and H. Kang, "A backstepping global fast terminal sliding mode control for trajectory tracking control of industrial robotic manipulators," *IEEE Access*, vol. 9, pp. 31 921–31 931, 2021.

[12] H. Liu, J. Sun, J. Nie, and L. Zou, "Observer-based adaptive second-order non-singular fast terminal sliding mode controller for robotic manipulators," *Asian Journal of Control*, vol. 23, pp. 1845–1854, 2021.

[13] A. Levant, "Chattering analysis," *IEEE Transactions on Automatic Control*, vol. 55, pp. 1380–1389, 2010.

[14] Y. Golouje and S. Abtahi, "Chaotic dynamics of the vertical model in vehicles and chaos control of active suspension system via the fuzzy fast terminal sliding mode control," *Journal of Mechanical Science and Technology*, vol. 35, pp. 31–43, 2021.

[15] M. Homayounzade and A. Khademhosseini, "Disturbance observer-based trajectory following control of robot manipulators," *International Journal of Control, Automation and Systems*, vol. 17, pp. 203–211, 2019.

[16] S. Mobayen, S. Mostafavi, and A. Fekih, "Non-singular fast terminal sliding mode control with disturbance observer for underactuated robotic manipulators," *IEEE Access*, vol. 8, pp. 198 067–198 077, 2020.

[17] H. Khalil, "Extended high-gain observers as disturbance estimators," *SICE Journal of Control, Measurement, and System Integration*, vol. 10, pp. 125–134, 2017.

[18] D. Shi, J. Zhang, Z. Sun, G. Shen, and Y. Xia, "Composite trajectory tracking control for robot manipulator with active disturbance rejection," *Control Engineering Practice*, vol. 106, pp. 1–8, 2021.

[19] J. Zhai and Z. Li, "Fast-exponential sliding mode control of robotic manipulator with super-twisting method," *IEEE Transactions on Circuits and Systems II: Express Briefs*, vol. 69, pp. 489–493, 2021.

[20] J. Craig, *Introduction to Robotics: Mechanics and Control*. London, UK: Pearson Educacion, 2005.

[21] M. Krstic, P. Kokotovic, and I. Kanellakopoulos, *Nonlinear and Adaptive Control Design*. Hoboken, NJ: John Wiley & Sons, Inc., 1995.

[22] M. Al Janaideh, A. M. Boker, and M. Rakotondrabe, "Output-feedback control of precision motion systems with uncertain nonlinearities," *Mechanical Systems and Signal Processing*, vol. 153, pp. 1–20, 2021.

[23] H. Khalil, *High-gain Observers in Nonlinear Feedback Control*. Philadelphia, PA: SIAM, 2017.

[24] Quanser, *QArm Instructor Manual*, 2022.